J Biomol NMR (2008) 42:209–223
DOI 10.1007/s10858-008-9278-7

ARTICLE

Effect of local sugar and base geometry on ^{13}C and ^{15}N magnetic shielding anisotropy in DNA nucleosides

Eva Brumovská · Vladimír Sychrovský · Zuzana Vokáčová · Jiří Šponer · Bohdan Schneider · Lukáš Trantírek

Received: 12 September 2008 / Accepted: 17 September 2008 / Published online: 14 October 2008

Abstract Density functional theory was employed to study the dependence of ^{13}C and ^{15}N magnetic shielding tensors on the glycosidic torsion angle (χ) and conformation of the sugar ring in 2′-deoxyadenosine, 2′-deoxyguanosine, 2′-deoxycytidine, and 2′-deoxythymidine. In general, the magnetic shielding of the glycosidic nitrogens and the sugar carbons was found to depend on both the conformation of the sugar ring and χ. Our calculations indicate that the magnetic shielding anisotropy of the C6 atom in pyrimidine and the C8 atom in purine bases depends strongly on χ. The remaining base carbons were found to be insensitive to both sugar pucker and χ re-orientation. These results call into question the underlying assumptions of currently established methods for interpreting residual chemical shift anisotropies and ^{13}C and ^{15}N auto- and cross-correlated relaxation rates and highlight possible limitations of DNA applications of these methods.

Keywords Magnetic shielding · Chemical shift anisotropy · DNA · RNA

Electronic supplementary material The online version of this article (doi:10.1007/s10858-008-9278-7) contains supplementary material, which is available to authorized users.

E. Brumovská · L. Trantírek (✉)
Faculty of Science, University of South Bohemia and Biology Centre AS CR v.v.i., Branišovská 31, 370 05 České Budějovice, Czech Republic
e-mail: trant@paru.cas.cz

V. Sychrovský · Z. Vokáčová
Institute of Organic Chemistry and Biochemistry, AS CR v.v.i., Flemingovo náměstí 2, 166 10 Prague, Czech Republic

J. Šponer
Institute of Biophysics, AS CR v.v.i., Královopolská 135, 612 65 Brno, Czech Republic

B. Schneider
Biotechnological Institute AS CR, Vídeňská 1083, 142 20 Prague, Czech Republic

Introduction

Knowledge of the magnitude and orientation of ^{13}C and ^{15}N magnetic shielding (MS)/chemical shift (CS) tensors in DNA and RNA nucleosides is essential for the interpretation of NMR relaxation data and for the analysis of residual chemical shift anisotropy (RCSA) resulting from weak alignment (Akke et al. 1997; Boisbouvier et al. 2000; Duchardt et al. 2004; Duchardt and Schwalbe 2005; Ferner et al. 2008; Grishaev et al. 2006; Hansen and Al-Hashimi 2006; Ravindranathan et al. 2003; Ravindranathan et al. 2005; Schofberger et al. 2006; Shajani and Varani 2007; Sychrovsky et al. 2005; Trantirek et al. 2007). Large chemical shift anisotropies (CSAs) of ^{13}C and ^{15}N nuclei in nucleic acids have been found useful for constraining bases relative to the molecular alignment tensor (Grishaev et al. 2006; Hansen and Al-Hashimi 2006), glycosidic torsion angle (Duchardt et al. 2004), sugar ring conformation (Boisbouvier et al. 2000), and the evaluation of conformational dynamics around a glycosidic bond (Ravindranathan et al. 2003). Until quite recently, the only available experimental data on the ^{13}C and ^{15}N CS-tensor magnitude and orientation in nucleic acids originated from solid-state NMR measurements and were limited to model compounds such as nucleic acid bases (Hu et al. 1998) or nucleosides (Stueber and Grant 2002).

In a recent report, Duchardt and Schwalbe simultaneously analyzed relaxation measurements for all protonated base carbons in the nucleosides of a small RNA hairpin, using

solid-state CSA values from Stueber and Grant (2002) (Duchardt and Schwalbe 2005). They found that the use of CSA values obtained from solid-state NMR measurements led to the remarkable result of systematically lower order parameters for the purine C8 atom compared to pyrimidine C6 sites, even for base paired nucleotides. They also reported that relaxation data recorded for ^{13}C and ^{15}N in the same nucleotide revealed a mismatch in the commonly used CSA values, and raised a question as to whether CSA values in solution NMR require adjustment from solid-state values.

Very recently, ^{13}C chemical shift anisotropies in right-handed double-helical DNA and RNA fragments were characterized in solution using the dependence of the relaxation rates on the magnetic field (Ying et al. 2006a), cross-correlated relaxation rates (Ravindranathan et al. 2005), and liquid crystal measurements (Bryce et al. 2005; Hansen and Al-Hashimi 2006; Ying et al. 2006b). Differences of up to 30 ppm were found between CSA values obtained from solid-state and solution NMR measurements. It was suggested that the different ^{13}C chemical shift anisotropies stemmed from differences in hydration of Watson–Crick base-paired oligonucleotides, molecular geometry, and electrostatic crystal potential (Stueber and Grant 2002; Ying et al. 2006b). It is generally recognized that the CS tensors of ^{1}H, ^{13}C, ^{15}N, and ^{31}P nuclei in nucleotides depend on local conformation (Dejaegere and Case 1998; Ebrahimi et al. 2001; Precechtelova et al. 2007; Sitkoff and Case 1998; Sychrovsky et al. 2005) and hydrogen bonding (Czernek et al. 2000). Dejaegere and Case (1998) reported calculations of MS tensors for methyl β-D-2′-deoxyribofuranoside and methyl β-D-ribofuranoside as models for the 2′-deoxyribose and ribose sugars in nucleic acids and found that the magnetic shielding anisotropies (MSA) for C1′ and C3′ are sensitive to puckering of the sugar ring. The dependence of the C1′ and C3′ MS tensors on sugar pucker in RNA polynucleotides was later confirmed experimentally by Boisbouvier et al. (2000). Recently, Sychrovsky et al. (2005) reported calculations of the C1′ and N1/9 MS-tensors in DNA nucleosides. They demonstrated that both the magnitude and orientation of C1′ and N1/9 MS tensors depend on the glycosidic torsion and sugar ring conformation and that accounting for conformation-dependent variability in these tensors may be crucial for proper interpretation of cross-correlated relaxation rates between the N1/9 CS-tensor and C1′–H1′ dipole–dipole interaction in nucleic acids. Importantly, these studies indicated that variations in MSA values due to differences in local molecular geometry may be two to three times larger than those due to the environmental differences experienced by nucleic acids in the solid and solution states.

Recent improvements in spectrometer hardware and measurement strategies permit the MS-tensor-related NMR parameters to be measured at levels of accuracy where their quantitative interpretation is limited by an unknown degree of site-to-site MS tensor variation. Due to a lack of information about ^{13}C and ^{15}N MS-tensors outside the right-handed double helical region, the quantitative interpretation of MS-tensor related NMR parameters in non-canonical regions, left-handed double helices, or multi-strand forms of DNA should be avoided as it might lead to structural errors (Sychrovsky et al. 2005). Mapping conformational dependencies of ^{13}C and ^{15}N MS-tensors in DNA is therefore valuable as it allows MS-tensor related NMR parameters to be used for structural analysis of biologically important nucleic acid motifs such as Z-DNA, DNA triplexes and quadruplexes, or unusual DNA duplex and hairpin motifs.

In the present study, we employed density functional theory (DFT) to investigate the relationships between the anisotropy of ^{13}C and ^{15}N MS and the sugar ring conformations and glycosidic torsion angle in 2′-deoxyadenosine, 2′-deoxyguanosine, 2′-deoxythymidine, and 2′-deoxycytidine. The main objectives were (1) to determine the range of individual principal components of the tensor for the experimentally observed sugar puckers and glycosidic bond orientation, and (2) to determine the changes in MS tensor orientations resulting from changes in sugar pucker and glycosidic bond conformation.

Methods

The compounds 2′-deoxyadenosine (dAde), 2′-deoxyguanidine (dGua), 2′-deoxycytidine (dCyt), 2′-deoxythymidine (dThy) (Fig. 1) were used as models for all calculations of the ^{13}C and ^{15}N MS tensors. The geometry of all nucleosides was gradient optimized with the B3LYP exchange-correlation functional (Becke 1993; Lee et al. 1988) and the 6-31G(d,p) atomic basis set. In the initial geometry optimization, the χ torsion angle was estimated to be close to either *syn* or *anti* minima (the *anti* region was defined as: $180° < \chi < 280°$, and *syn* as $50° < \chi < 80°$), and the sugar was adjusted to either C3′-endo (Pseudorotation angle P (Altona and Sundaralingam 1972) set to approximately 20°) or C2′-endo (P about 160°). A constrained geometry optimization for a stepwise change in torsion angle χ was then performed for each nucleoside. All parameters were freely optimized except χ. The magnetic shielding tensors were calculated using the GIAO approach (Wolinski et al. 1990) with the B3LYP functional and the atomic basis set (9s,5p,1d/5s,1p)[6s,4p,1d/3s,1p] for both carbon and nitrogen (Kutzelnigg et al. 1991). All calculations were performed with the Gaussian G03 program (Frisch et al. 2004).

A second-rank MS tensor in the principal axis system was obtained from the NMR calculations. The full

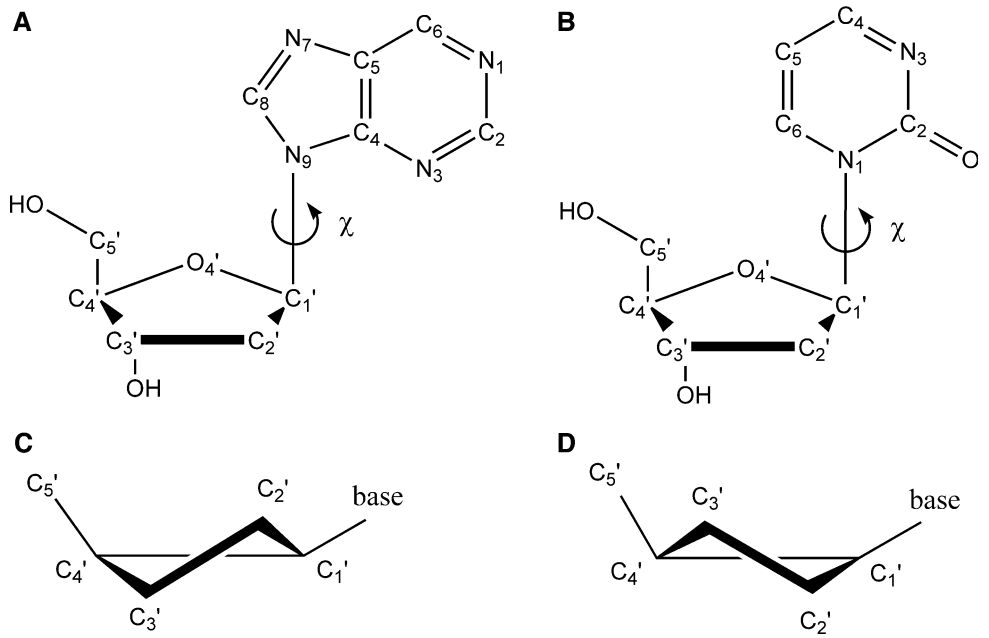

Fig. 1 Structure and atom numbering scheme for **a** 2′-deoxypurine and **b** 2′-deoxypyrimidine. Carbon and nitrogen atoms are numbered according to IUPAC nomenclature (Markley et al. 1998). The glycosidic torsion angle χ is defined by atoms O4′–C1′–N9–C4 in purines and O4′–C1′–N1–C2 in pyrimidines. There are two energetically favored regions of χ, *anti* and *syn*. In agreement with comparative studies of crystallographic data, the *anti* region is defined as $180° < \chi < 280°$, and the *syn* region as $50° < \chi < 80°$. **c** and **d** Schematic representations of the two main sugar conformations in DNA, C2′-endo (Pseudorotation angle P (Altona and Sundaralingam 1972) approximately 160°) and C3′-endo (P about 20°)

MS tensor was decomposed into its isotropic and anisotropic (herein, referred to as MSA tensor) parts. A traceless MSA tensor in the principal axis system is described by two adjustable parameters: its magnitude $|\sigma^{M}| = \left(\sigma_x^2 + \sigma_y^2 - \sigma_x\sigma_y\right)^{1/2}$, where $\sigma_x = \sigma_{11} - \sigma_{33}$ and $\sigma_y = \sigma_{22} - \sigma_{33}$, and its asymmetry, $\eta = (\sigma_{22} - \sigma_{11})/\sigma_{33}$, where $\sigma_{11} \leq \sigma_{22} \leq \sigma_{33}$.

Results

Dependence of MSA on sugar pucker and glycosidic torsion angle

Base nitrogens

The calculated nitrogen MSA tensor magnitudes and orientations as a function of the sugar pucker and glycosidic torsion angle (χ) for pyrimidine and purine 2′-deoxynucleosides are displayed in Figs. 2 and 3, respectively. The MSA tensors of the base nitrogen atoms are almost independent of the sugar pucker with the exception of the N1 pyrimidine and N9 purine atoms involved in the glycosidic bond. Their MSA tensors depend on both orientation of the glycosidic bond and sugar pucker. While the magnitudes $|\sigma^{M}|$ of the glycosidic nitrogen MSA tensors in 2′-deoxypyrimidines in the *syn* conformation are essentially the same for the C2′-and C3′-endo sugar puckers, our calculations indicate that sugar pucker mode has a pronounced influence on $|\sigma^{M}|$ values in the *anti* region. For *anti* 2′-deoxypyrimidines with C3′-endo sugars, the absolute values of $|\sigma^{M}|$ are expected to be 10–12 ppm larger than $|\sigma^{M}|$ values for *anti* 2′-deoxypyrimidines with C2′-endo sugars. For 2′-deoxythymidine, asymmetry of the glycosidic nitrogen MSA tensor is independent of the conformation of the sugar ring. In contrast, asymmetry of the tensor in 2′-deoxycytidine depends on sugar pucker mode. For both *syn* and *anti* 2′-deoxycytidine with C3′-endo sugars, the absolute values of η are predicted to be smaller by 0.2–0.25 than those of 2′-deoxycytidine with C2′-endo sugars. In general, the conformation of the glycosidic bond and sugar pucker has only a moderate effect on the orientation of the glycosidic nitrogen MSA tensor. The most pronounced effect has been found for the N1 atom of 2′-deoxycytidine in the *anti* conformation. The orientation of σ_{11}, in *anti* 2′-deoxycytidine with a C2′-endo sugar differs from the orientation observed in *anti* 2′-deoxycytidine with a C3′-endo sugar by $\sim 15°$.[1]

[1] The data for the N1/9 were obtained in our previous study (supplementary material) (Sychrovsky et al. 2005).

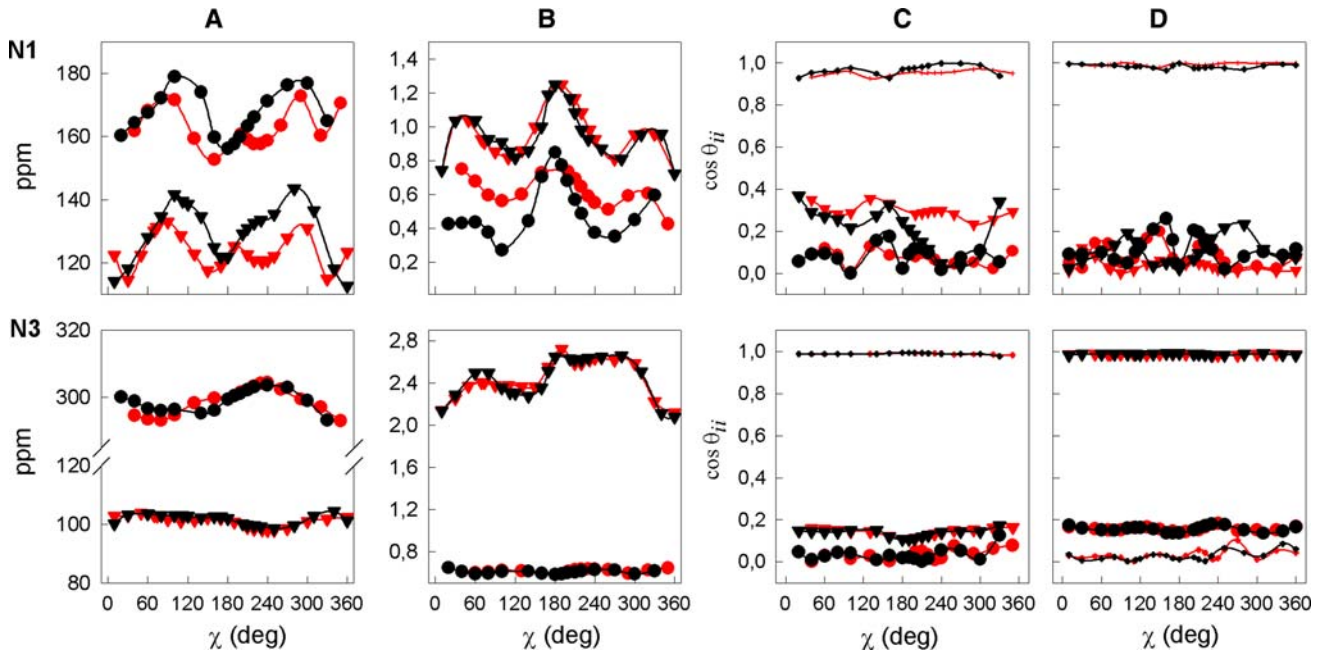

Fig. 2 Calculated magnitudes $|\sigma^{M}|$ (**a**) and asymmetries η (**b**) of ^{15}N MSA tensors for 2′-deoxycytidine (-●-) and 2′-deoxythymidine (-▼-) as a function of glycosidic torsion angle χ in C2′-endo (in *red*) and C3′-endo (in *black*) conformation. **c** and **d** display the calculated orientation (θ_{11}(▼),θ_{22}(•),θ_{33}(●)) of individual components of the MSA tensor with respect to the N1–C2 bond as a function of torsion angle χ in C2′-endo (in *red*) and C3′-endo (in *black*) sugar conformation in 2′-deoxycytidine and 2′-deoxythymidine, respectively. The orientations are expressed in absolute values of cos θ_{ii}. The data for N1 were obtained in our previous study (supplementary material) (Sychrovsky et al. 2005)

In 2′-deoxypurines, the sugar pucker mode has negligible influence on the $|\sigma^{M}|$ or η values and orientations of the N1, N3, and N7 MSA tensors (Fig. 3). However, analogous to the 2′-deoxypyrimidines, sugar pucker mode strongly influences the glycosidic nitrogen MSA tensor magnitude and shape as well as its orientation with respect to the base geometry. While the magnitudes of the tensor in *syn* 2′-deoxypurines are independent of sugar pucker mode, the differences in $|\sigma^{M}|$ values between C2′-endo and C3′-endo sugar puckers reaches up to 12 ppm in the *anti* region. For *syn* 2′-deoxypurines with C2′-endo sugar puckers, the absolute value of η is reduced by 0.1 compared to 2′-deoxypurines with C3′-endo sugar puckers. For *anti* 2′-deoxypurines, the corresponding difference ranges up to 0.35. In addition, our calculations indicate that when sugar pucker changes from C2′-endo to C3′-endo, the glycosidic nitrogen MSA tensor reorients itself by about 15°.

Base carbons

The calculated base carbon MSA tensor magnitudes, asymmetries and orientations as a function of the sugar pucker and glycosidic torsion angle for pyrimidine and purine 2′deoxynucleosides are depicted in Figs. 4 and 5, respectively. In general, the MSA tensors of the base carbon atoms exhibited negligible dependence on sugar pucker. As expected, our analysis indicated that the MSA tensors of the quaternary 2′-deoxypyrimidine C4 atoms are not influenced by the orientation of the glycosidic bond, in contrast to the carbon atoms proximal to the glycosidic linkage (i.e. C2, C6 and to some extent C5). While differences in $|\sigma^{M}|$ of the C5 atom MSA tensors between *syn* and *anti* conformations are only about 5 ppm, the corresponding difference for C6 atoms can be as great as 20–25 ppm. In 2′-deoxypyrimidines, the C2 MSA tensor $|\sigma^{M}|$ and η values are modulated by the orientation of the glycosidic bond (Fig. 4). The differences in absolute values of $|\sigma^{M}|$ and η between syn and anti conformations are about 10 ppm and 0.3. In addition, the C2 MSA tensor asymmetry η is influenced by the conformation of the sugar ring. However, the absolute η values for C2′-endo and C3′-endo sugar pucker are essentially the same in both syn and anti regions. Our calculations indicate that the η and cos σ_{ii} values of the C4 and C5 MSA tensors are quite insensitive to reorientation of the glycosidic torsion angle. In contrast to the C6 MSA tensor orientation, the asymmetry of the tensor is substantially modulated by χ. The difference between C6 η values corresponding to the *syn* and *anti* conformations is about 0.5.

The MSA tensors of the base carbons in 2′-deoxypurines appeared to be essentially independent of χ with the exception of the C8 atoms (Fig. 5). Although the

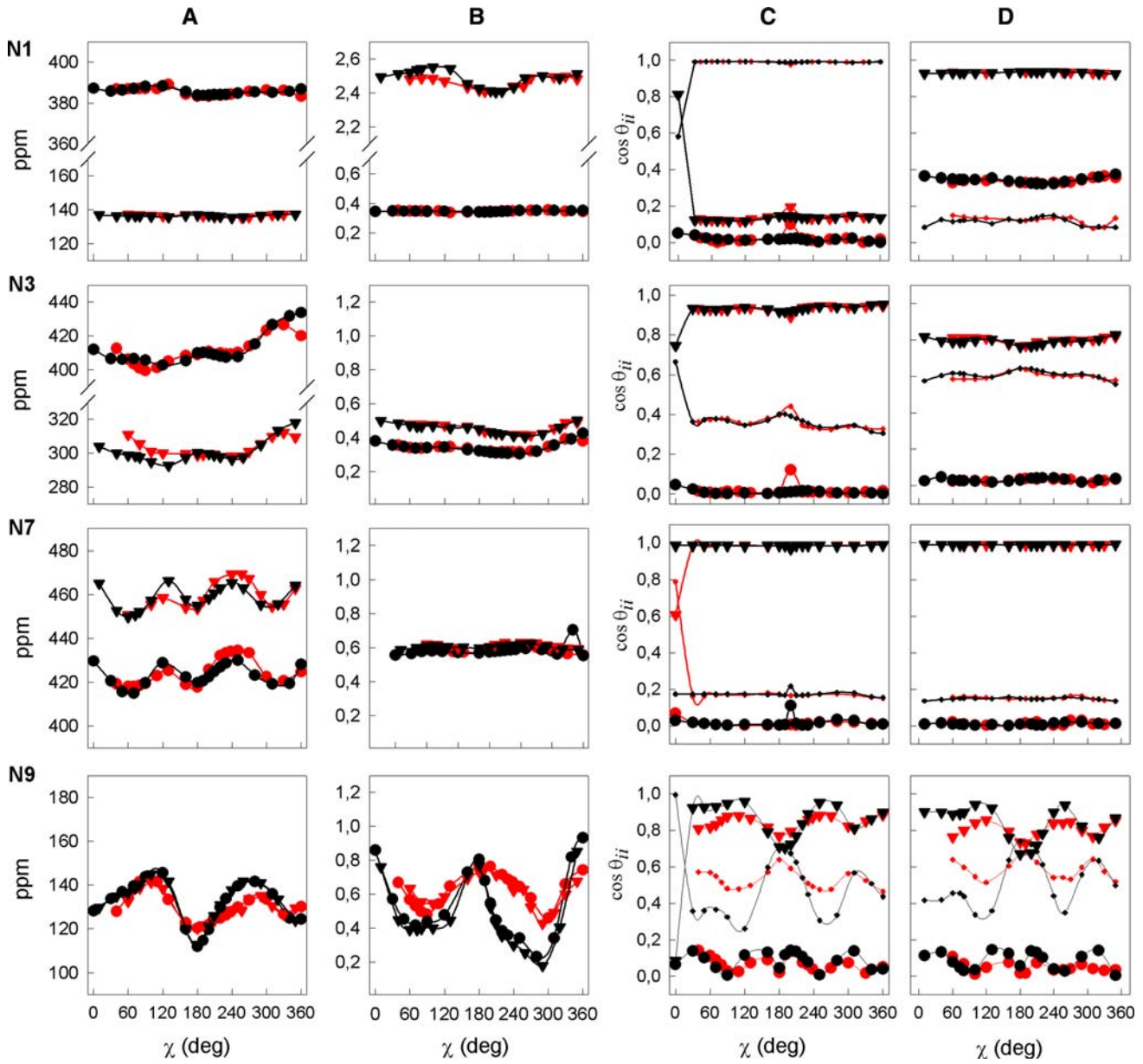

Fig. 3 Calculated magnitudes $|\sigma^{M}|$ (**a**) and asymmetries η (**b**) of ^{15}N MSA tensors for 2′-deoxyadenine (-●-) and 2′-deoxyguanosine (-▼-) as a function of glycosidic torsion angle χ in C2′-endo (in *red*) and C3′-endo (in *black*) conformation. **c** and **d** display the calculated orientation (θ_{11}(▼),θ_{22}(•),θ_{33}(●)) of individual components of the MSA tensor with respect to the N9–C4 bond as a function of torsion angle χ in C2′-endo (in red) and C3′-endo (in *black*) sugar conformation in 2′-deoxyadenosine and 2′-deoxyguanosine, respectively. The orientations are expressed in absolute values of cos θ_{ii}. The data for N9 were obtained in our previous study (supplementary material) (Sychrovsky et al. 2005)

conformation of χ clearly does not influence orientation of the C8 MSA tensor, it has a pronounced influence on both $|\sigma^{M}|$ and η. For 2′-deoxyadenosine, the differences in the absolute values of $|\sigma^{M}|$ and η between the *syn* and *anti* conformation are about 12 ppm and 0.6, respectively. For 2′-deoxyguanosine, the corresponding differences are about 10 ppm and 0.8. Although the C4 and C5 MSA tensor $|\sigma^{M}|$ and η values appear to be modulated by orientation of the glycosidic bond, the absolute values of $|\sigma^{M}|$ and η are essentially the same in the stereochemically important regions of χ. The orientations of the C4 MSA tensors in 2′-deoxypurines are independent of χ. It is worth mentioning (see "Discussion") that while the orientation of the C5 MSA tensor in 2′-deoxyguanosine is independent of the glycosidic bond angle, our calculations indicate that the C5 MSA tensor of 2′-deoxyadenosine differs slightly in orientation between the *syn* and *anti* regions.

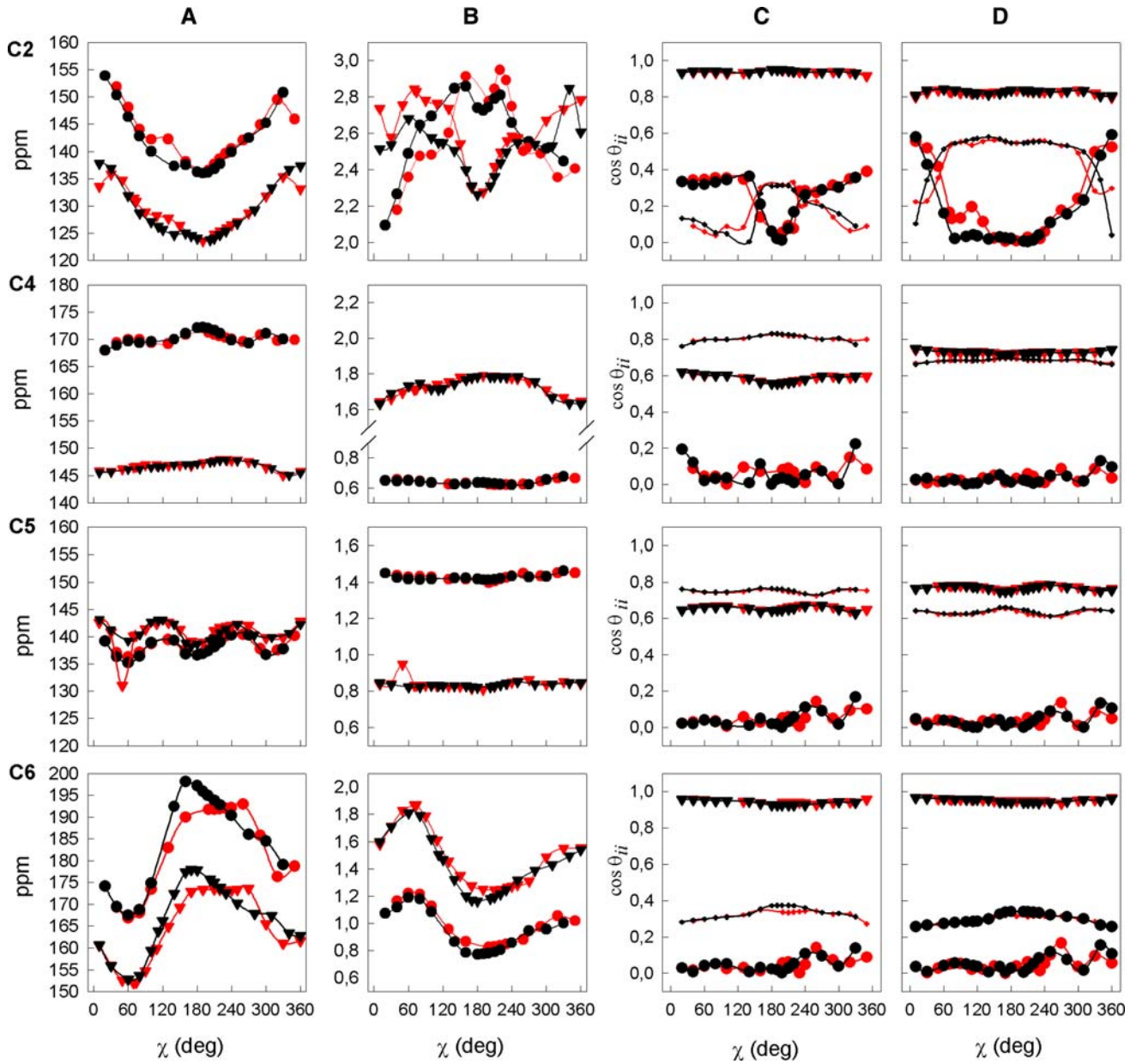

Fig. 4 Calculated magnitudes $|\sigma^{M}|$ (**a**) and asymmetries η (**b**) of base ^{13}C MSA tensors for 2′-deoxycytidine (-●-) and 2′-deoxythymidine (-▼-) as a function of glycosidic torsion angle χ in C2′-endo (in *red*) and C3′-endo (in *black*) conformation. **c** and **d** display the calculated orientation (θ_{11}(▼),θ_{22}(•),θ_{33}(●)) of individual components of the MSA tensor with respect to the N1–C2 bond as a function of torsion angle χ in C2′-endo (in *red*) and C3′-endo (in *black*) conformation in 2′-deoxycytidine and 2′-deoxythymidine, respectively. The orientations are expressed in absolute values of cos θ_{ii}

Sugar carbons

Figures 6 and 7 depict the calculated magnitudes, asymmetries, and orientations for the MSA tensors of sugar carbons in 2′-deoxypyrimidines and 2′-deoxypurines, respectively. As anticipated, the MSA tensors of all endocyclic sugar carbons are significantly affected by the sugar pucker mode. In 2′-deoxypyrimidines, the orientation of the glycosidic torsion angle has only a small influence on the MSA tensor with exception of the C1′ and C2′ carbon atoms. Noteworthy, the $|\sigma^{M}|$ of the C1′ MSA changes up to 25 ppm upon re-orientation of the torsion angle χ between *syn* and *anti* regions.[2] The quantity most sensitive to the sugar pucker mode is the magnitude of the C3′ carbon MSA tensor. The difference in the absolute value of $|\sigma^{M}|$ between C2′- and C3′-endo sugar conformations can be up

[2] The data for C1' were obtained in our previous study (supplementary material) (Sychrovsky et al. 2005).

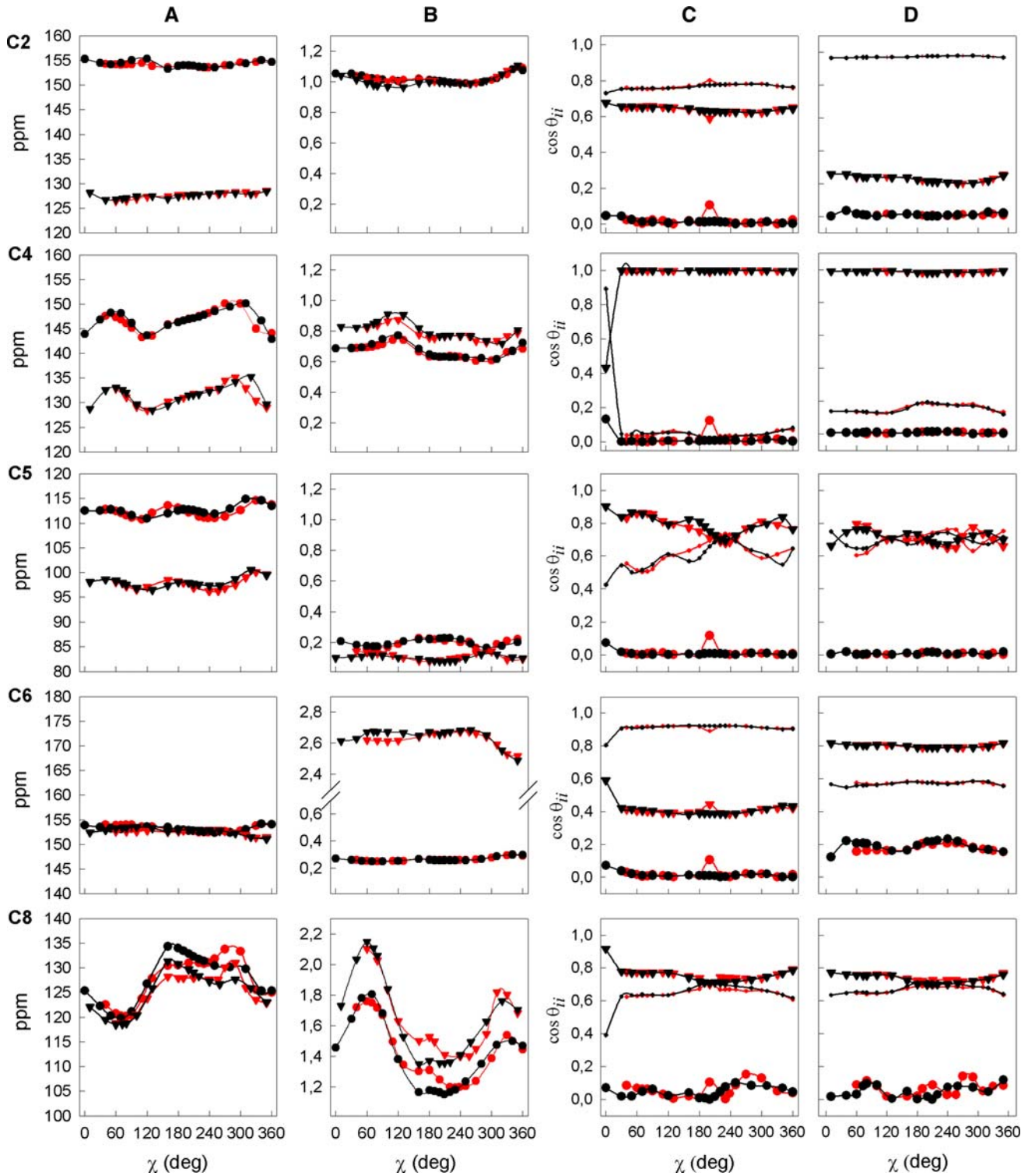

Fig. 5 Calculated magnitudes $|\sigma^{M}|$ (**a**) and asymmetries η (**b**) of base ^{13}C MSA tensors for 2′-deoxyadenosine (-●-) and 2′-deoxyguanosine (-▼-) as a function of glycosidic torsion angle χ in C2′-endo (in *red*) and C3′-endo (in *black*) conformation. **c** and **d** display the calculated orientation (θ_{11}(▼),θ_{22}(•),θ_{33}(●)) of individual components of the MSA tensor with respect to the N9–C4 bond as a function of torsion angle χ in C2′-endo (in *red*) and C3′-endo (in *black*) conformation in 2′-deoxyadenosine and 2′-deoxyguanosine, respectively. The orientations are expressed in absolute values of cos θ_{ii}

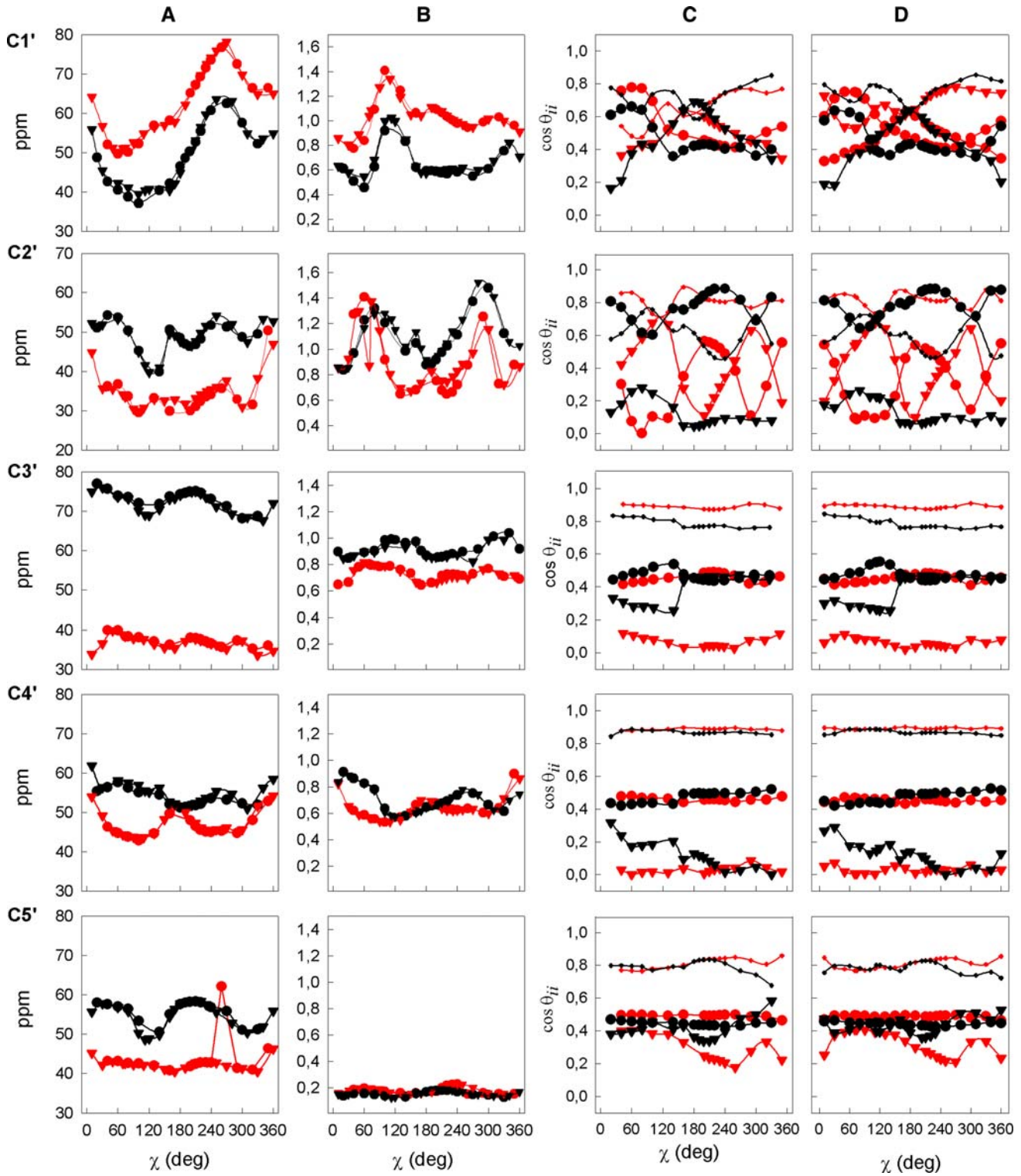

Fig. 6 Calculated magnitudes $|\sigma^{M}|$ (**a**) and asymmetries η (**b**) of sugar ^{13}C MSA tensors for 2′-deoxycytidine (-●-) and 2′-deoxythymidine (-▼-) as a function of glycosidic torsion angle χ in C2′-endo (in *red*) and C3′-endo (in *black*) conformation. **c** and **d** display the calculated orientation (θ_{11}(▼),θ_{22}(•),θ_{33}(●)) of individual components of the MSA tensor for C1′, C2′, C3′, C4′, and C5′ carbons with respect to the C1′–N1/9, C1′–C2′, C2′–C3′, C3′–C4′, and C4′–C5′ bonds for 2′-deoxycytidine and 2′-deoxythymidine, respectively. The orientations are expressed in absolute values of cos θ_{ii}. See footnote 2

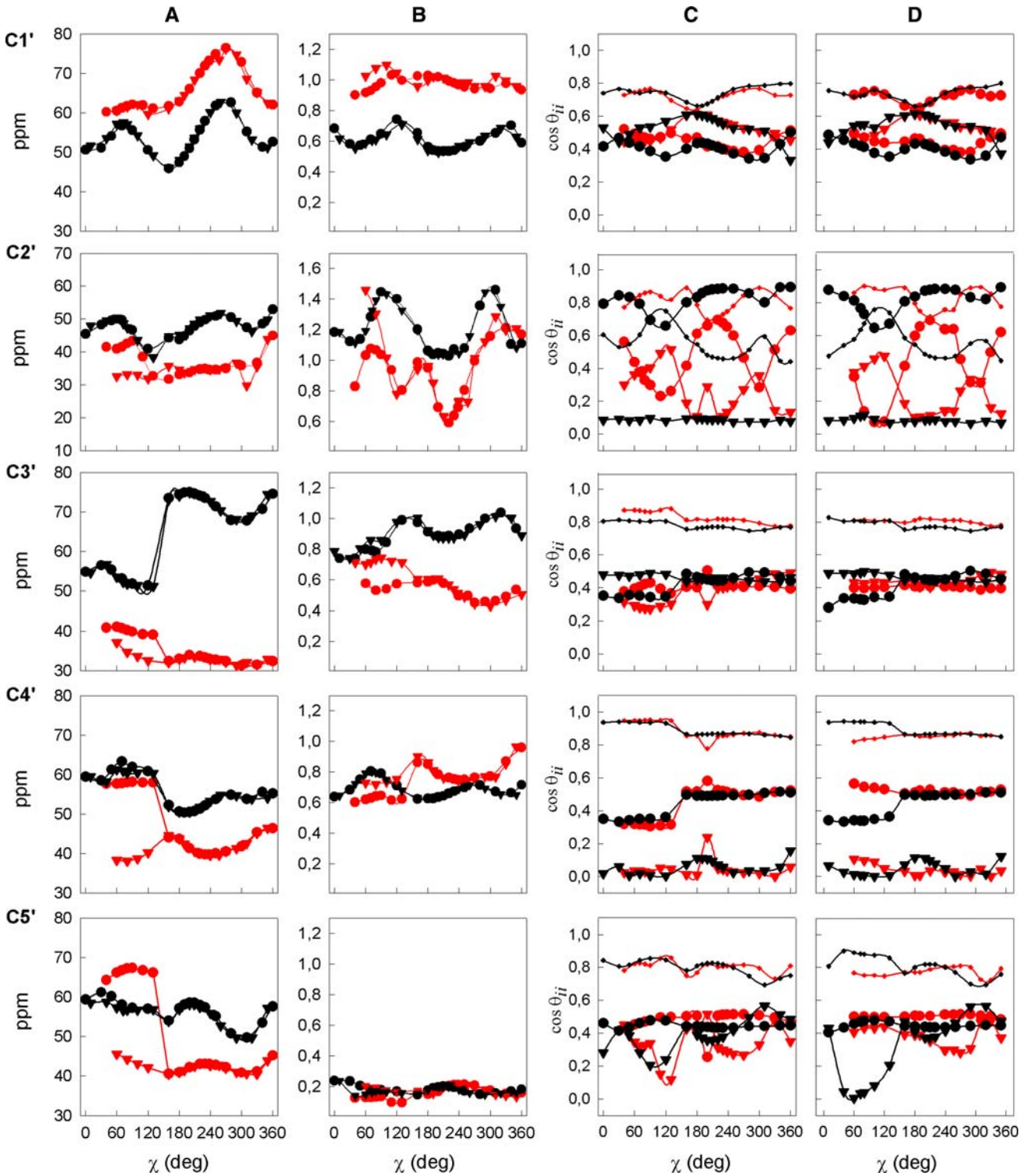

Fig. 7 Calculated magnitudes $|\sigma^{M}|$ (**a**) and asymmetries η (**b**) of sugar ^{13}C MSA tensors for 2′-deoxyadenosine (-●-) and 2′-deoxyguanosine (-▼-) as a function of glycosidic torsion angle χ in the C2′-endo (in *red*) and C3′-endo (in *black*) conformation. **c** and **d** display the calculated orientation (θ_{11}(▼),θ_{22}(•),θ_{33}(●)) of individual components of the MSA tensor for C1′, C2′, C3′, C4′, and C5′ carbon atoms with respect to the C1′–N1/9, C1′–C2′, C2′–C3′, C3′–C4′, and C4′–C5′ bonds for 2′-deoxyadenosine and 2′-deoxyguanosine, respectively. The orientations are expressed in absolute values of cos θ_{ii}. See footnote 2

to 35 ppm. The corresponding differences for the other sugar carbon atoms range from 10 to 22 ppm.

The MSA tensors of the endo-cyclic sugar carbons in 2′-deoxypurines display a pattern of conformational dependence similar to the 2′-deoxypyrimidines. However, in contrast to the 2′-deoxypyrimidines, the $|\sigma^{M}|$ values of the C3′, C4′, and C5′ MSA tensors in 2′-deoxypurines are sensitive to reorientation of the glycosidic torsion angle. In syn 2′-deoxyguanosine with C3′-endo sugar, the N3 gets close to H3′ (~2.5 Å). This might affect the C3′ MSA. Similarly, in syn 2′-deoxypurines with C2′-endo sugars, the N3 get close to the H5′ (~2.8 Å). In this case, a weak interaction between electron cloud from the N3 and H5′ might affect the C5′ MSA. The C5′ MSA is sensitive to reorientation of the glycosidic torsion angle only in 2′-deoxyguanosine, but not in 2′-deoxyadenosine. The explanation for this may be in pronouncedly lower electron density at the N3 of 2′-deoxyadenosine as compared to the N3 of 2′-deoxyguanosine. The C4′ MSA seems to be affected indirectly. The effect appears to be coupled with weak contact formation between the N3 of 2′-deoxyguanosine and its H5′.

Basis set dependence of DFT calculations

The choice of atomic basis for MS calculation may affect the accuracy of the modeled MSA tensor (Schofberger et al. 2006; Sitkoff and Case 1998; Stueber and Grant 2002). To estimate the basis set effect, we performed calculations of the $|\sigma^{M}|$ with the Iglo II and a larger Iglo III basis for the selected grid point geometries of 2′-deoxyguanosine (Fig. 8). For *syn* ($\chi = 40°…110°$, supplementary material) 2′-deoxyguanosine with C2′-endo sugar pucker, the absolute differences between the $|\sigma^{M}|$ values of CSA tensors calculated with the Iglo II and Iglo III basis sets range between 4.6 and 4.9 ppm. For the energy optimum in the *syn* region, the absolute difference between $|\sigma^{M}|$ values calculated with Iglo II and Iglo III were 4.62 and 4.61 ppm for the C2′-endo ($\chi = 68.8°$) and C3′-endo ($\chi = 72.8°$) sugar pucker, respectively. The effect of atomic basis on the magnitude of C8 MSA tensors of $\sim 4.8 \pm 0.2$ ppm remains essentially constant along the geometry variation carried out for the structural descriptor χ and, furthermore, is independent of sugar pucker.

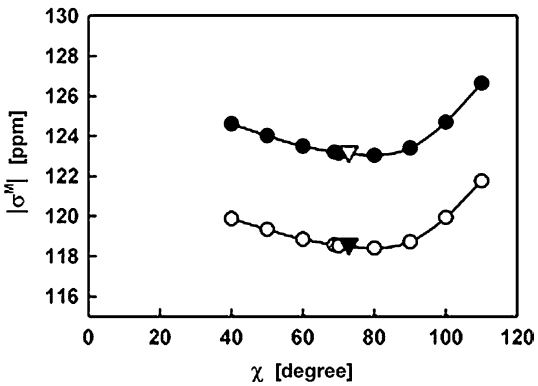

Fig. 8 Comparison of the $|\sigma^{M}|$ values for C8 MSA tensors calculated using the Iglo II (*open circles*) and Iglo III (*filled circles*) basis sets. The values were calculated for 2′-deoxyguanosine with C2′-endo sugar pucker and $\chi = 40°$, 50°, 60°, 68.8°, 70°, 80°, 90°, 100° and 110°. The *open* and *filled triangles* correspond to σ^{M} values for the C8 MSA tensors calculated for energy optima (C2′-endo, $\chi = 68.8°$ and C3′-endo, $\chi = 72.8°$) with the Iglo II and Iglo III basis sets, respectively

Discussion

Correlation between experimental and calculated shielding values

In 2006, base carbon CSA values obtained by liquid-crystal NMR and solution relaxation measurements were reported for a double helical A-form RNA segment and a double helical B-form DNA dodecamer (Ying et al. 2006b). These CSA values differ notably from the previous values obtained by solid-state NMR (Stueber and Grant 2002) with changes up to 30 ppm. Table 1 contains a comparison of calculated and experimental $|\sigma^{M}|$ and η values for base carbons in 2′-deoxyribonucleosides/ribonucleosides. In general, the MSA values calculated in this study were found to be in very good agreement with solid-state NMR results on mono-nucleosides. While calculated $|\sigma^{M}|$ values differ by an average of about 4.5 ± 4.3 ppm from experimental $|\sigma^{M}|$ values as determined by solid-state measurements, the corresponding differences between the calculated values and those obtained by liquid-crystal NMR and solution relaxation measurements are approximately 7.9 ± 4.5 ppm. The largest difference is observed for C2 in 2′-deoxyadenosine (up to 15 ppm). However, this difference primarily reflects the fact that our calculations, similarly to the solid-state NMR measurements, do not include the effects of base-pairing. It is well known that the change of the isotropic chemical shift of C2 between base-paired and free adenosine is up to 7 ppm. It follows that the solution values for C2 by Ying et al. (2006b) and those from solid-state by Stueber and Grant and our calculations cannot be directly compared. Considering that the calculated $|\sigma^{M}|$ values for base carbons are systematically underestimated by approximately 4 ppm (see "Results") due to application of the Iglo II basis in the calculations, we find a very good agreement between the calculated and solution data obtained by liquid-crystal NMR on an A-form RNA and a B-form DNA fragment. It is important to emphasize that while the differences between CSA/MSA values obtained using different approaches are usually less

Table 1 Comparison of $|\sigma^M|$ and η values for nucleoside base carbon CS/MS tensors determined by: quantum chemical calculations (DFT), solid state NMR spectroscopy (SS) by Stueber and Grant (2002), NMR relaxation and liquid crystal measurements (REL/LC) by Ying et al. (2006b) and liquid crystal measurements (RCSA) by Hansen and Al-Hashimi (2006)

Atom	$\lvert\sigma^M\rvert^a$ (DFT)	$\lvert\sigma^M\rvert$ (SS)	$\lvert\sigma^M\rvert$ (REL/LC)	$\lvert\sigma^M\rvert$ (RCSA)	η^a (DFT)	η (SS)	η (REL/LC)	η (RCSA)
dA-C2	153.6	150*	168 ± 2	n.d.	0.99	0.92*	0.70 ± 0.03	n.d.
dC-C5	140.4	138*	144 ± 1	172.6 ± 21.2*	1.43	1.03*	0.95 ± 0.03	1.40*
dC-C6	192.1	179*	186 ± 3	n.d.	0.86	0.83*	0.67 ± 0.03	n.d.
dT-C6	173.3	170	168 ± 3	n.d.	1.27	1.17	1.02 ± 0.13	n.d.
dG-C8	127.7	126*	133 ± 1	148.1 ± 12.8*	1.4	0.92*	0.88 ± 0.05	2.22*
		134*				1.08*		
dA-C8	131.1	134*	144 ± 1	n.d.	1.2	1.04*	0.88 ± 0.05	n.d.

The values of $|\sigma^M|$ are given in [ppm]

* The data were derived for ribonucleosides or polyribonucleotides

[a] Calculated values obtained in this study taken from 2′deoxynucleosides with C2′-endo sugar pucker and $\chi \sim 240^\circ$

than 10 ppm, for some base carbons they may be 1.5–2 times larger due to their dependence on orientation of the glycosidic torsion angle χ.

While there is very good agreement among experimental CSA and calculated MSA magnitudes, the asymmetry values for the same CS/MS tensors are mostly very different. The definitions of the CS/MS tensor magnitude and asymmetry imply their different sensitivity towards variations in principal values of the CS/MS-tensor. In general, the asymmetry parameter is much more sensitive to variations of the CS/MS tensor eigenvalues as compared with the magnitude. For example, the magnitude of C6 CS tensor from 2′-deoxythymidine, as determined from solid-state NMR measurements, is 170 ppm, as compared with 168 ppm determined from relaxation measurements. The asymmetry from the solid-state is 1.17, as compared with 1.02 from measurements in solution. In this case, the difference in CS-tensor magnitudes is less than 1.2%, but the difference in the CS-tensor asymmetries is about 12.8%. This example illustrates that even small differences between two CS/MS tensor's eigenvalues might translate into large differences in calculated asymmetries. This makes the comparison between CSA tensors from various NMR experiments and/or MSA tensors from quantum chemical calculations by means of asymmetries problematic.

With the exception of cytidine, Ying et al. (2006b) observed that CSA values of base carbons for 2′-deoxyribonucleosides are essentially the same as for ribonucleosides. The similarity between $|\sigma^M|$ values for 2′-deoxyribonucleosides and ribonucleosides suggest that the base carbons in DNA and RNA might exhibit similar patterns of conformational dependence on sugar pucker and glycosidic torsion angle.

Recently, two independently developed methods suggested RCSAs resulting from weak alignment as a new long-range orientational constraint for NMR refinement of nucleic acid structure (Grishaev et al. 2006; Hansen and Al-Hashimi 2006). Both of these methods, Hansen's and Grishaev's, express the modulation of the absolute RCSA values as a product of the principal components of the CSA tensor and a simple geometric term relating the orientation of the principal axis of an alignment tensor and the principal axis of the CSA tensor of C2 and C8 purine and C5 and C6 pyrimidine atoms, respectively.

The fundamental assumption of both methods is that the base carbon MSA tensors are independent of molecular geometry. Since the dependence of base carbon MSA tensors on their local environment had not been previously investigated, the authors have suggested avoiding the application of these methods outside the canonical double-helical geometry as it might lead to structural errors (Grishaev et al. 2006). Indeed, our calculations show that the MSA tensor magnitudes and asymmetries of the pyrimidine C6 and purine C8 atoms are strongly modulated by orientation of the glycosidic torsion angle (Figs. 4 and 5), in contrast to the MSA tensor orientations. The differences in the MSA tensor magnitudes between the *syn* and *anti* conformations range from 15 to 25 ppm depending on the base type. Therefore, the method of Grishaev can lead to bias in cases where no a priori information about the conformation of the glycosidic torsion angle is available. Our calculations suggest that for *syn* nucleotides the use of the method might require adjustments of the principal values of the experimental carbon CSA tensors, which seem to be specific for *anti* nucleotides (supplementary material). While application of the Hansen and Grishaev methods to C6 and C8 carbons for syn nucleotides may require adjustment of CSA values, our calculation suggests that the application of these methods to quaternary carbons, C4 and C5 in purines and C4 in pyrimidines, should be straightforward. The magnitudes, asymmetries, and orientations of these quaternary base carbon MSA tensors are practically independent of molecular geometry and are not likely to be affected by base-pairing, in contrast to C2

MSA in pyrimidines and purines. With the recent progress in the detection of quarternary carbons in nucleic acids (Fiala et al. 2004; Fiala and Sklenar 2007), quarternary carbon RCSAs may become a valuable source of structural data.

In addition, our calculations suggest that the MSAs of C6 and C8 might be very useful in determining the glycosidic bond preferred conformation due to their strong dependency on χ. For example, simple measurements of cross-correlated relaxation rates between C6/8 CSA and C6/8–H6/8 dipole–dipole should provide unambiguous discrimination between the *syn* and *anti* nucleotides.

Table 2 shows comparison of $|\sigma^{M}|$ and η values for sugar carbon MSA tensors calculated for *anti* 2′-deoxynucleosides with experimental $|\sigma^{M}|$ and η values obtained from solid-state measurements on isolated cytidine, guanosine dihydrate, adenosine and 2′-deoxythymidine (Stueber and Grant 2002) or liquid-crystal NMR of A-form helical RNA (Bryce et al. 2005). The data by Stueber and Grant shows differences in sugar CSA tensors among individual nucleosides. However, as the molecular geometries of the nucleosides used for the measurements were unknown and the samples of individual nucleosides differed in preparation, it is not fully clear whether these differences reflect different base types, electrostatic crystal potential, influence of different counter ions or differences in molecular structure. In contrast to results by Stueber and Grant, a fundamental assumption in data analysis by Bryce et al. was that, due to the well-characterized uniformity of A-form RNA, all sugar carbons from the double helical A-type stem might be described by a single CSA tensor regardless of base type. Our calculations indicate that this assumption is also valid for 2′-deoxynucleosides in *anti* conformation. However, there are significant differences between purine and pyrimidine 2′-deoxynucleosides in the *syn* region (Figs. 6 and 7). For C1′, the differences between syn 2′-deoxypurines and 2′-deoxypyrimidines may be up to 15 ppm for C3′-endo and 10 ppm for C2′-endo sugar pucker. For C3′, the differences are even more pronounced, up to 20 ppm. This dependence of C1′ and C3′ MSAs in 2′-deoxypurines on torsion χ might adversely impact the sugar pucker analysis (Boisbouvier et al. 2000) (*vide* infra).

Table 2 Comparison of $|\sigma^{M}|$ and η values for nucleoside sugar carbon CS/MS tensors determined by: quantum chemical calculations (DFT), solid state NMR spectroscopy (SS) by Stueber and Grant (2002) and NMR liquid crystal measurements (LC) by Bryce et al. (2005)

		dAde/Ade		dGua/Gua		dCyt/Cyt		dThy/Thy	
		$\|\sigma^{M}\|$	η	$\|\sigma^{M}\|$	η	$\|\sigma^{M}\|$	η	$\|\sigma^{M}\|$	H
C1′	DFT[a]	70.1	1.01	68.3	0.98	69.3	1.04	69.7	1.04
	DFT[b]	55.7	0.53	56.0	0.55	55.5	0.57	56.6	0.60
	SS	28.6*	1.04*	50.6*	0.74*	31.2*	1.31*	65.0	0.88
	LC	30.2*	1.11*						
C2′	DFT[a]	34.6	0.59	34.6	0.64	34.2	0.65	34.1	0.75
	DFT[b]	49.0	1.03	49.8	1.04	48.3	1.03	49.7	1.04
	SS	54.0*	0.76*	52.0*	0.91*	26.1*	0.68*	33.8	1.03
	LC	23.9*	0.85*						
C3′	DFT[a]	33.6	0.57	33.5	0.55	37.6	0.70	37.4	0.73
	DFT[b]	74.1	0.87	74.4	0.89	74.7	0.86	74.6	0.87
	SS	25.5*	0.63*	31.4*	0.72*	58.3*	0.68*	32.4	0.43
	LC	83.1*	0.84*						
C4′	DFT[a]	39.9	0.76	40.5	0.76	45.6	0.64	45.4	0.62
	DFT[b]	51.3	0.66	51.8	0.67	52.2	0.69	52.9	0.70
	SS	57.7*	0.55*	42.3*	0.60*	61.8*	0.52*	47.7	0.88
	LC	83.5*	1.08*						
C5′	DFT[a]	43.1	0.20	42.4	0.19	42.8	0.22	43.0	0.22
	DFT[b]	58.0	0.20	57.5	0.20	58.1	0.18	58.3	0.19
	SS	45.7*	0.63*	39.1*	0.80*	48.5*	0.65*	45.0	0.60
	LC	57.2*	0.23*						

The values of $|\sigma^{M}|$ are given in [ppm]

* The data were derived for ribonucleosides or polyribonucleotides

[a] Calculated values obtained in this study taken from 2′deoxynucleosides with C2′-endo sugar pucker and $\chi \sim 220^{\circ}$

[b] Calculated values obtained in this study taken from 2′deoxynucleosides with C3′-endo sugar pucker and $\chi \sim 220^{\circ}$

Pronounced differences in $|\sigma^{M}|$ values from the RCSA analysis compared with the other methods (DFT, SS, and REL/LC) are observed (Table 1). As discussed in the original report on RCSA analysis by Hansen and Al-Hashimi, these differences might represent an artifact of the RCSA procedure that follows uniform CSA values site to site, bond lengths r_{CH}(base) = 1.08 Å and $r_{C1'-H1'}$(sugar) = 1.09 Å, and that internal motions uniformly scale all of the measured residual dipolar couplings (RDCs) and RCSAs by a similar amount. As none of these assumptions is entirely valid for polyribonucleotides, the overestimated $|\sigma^{M}|$ values as compared with solid-state measurements by Stueber and Grant, relaxation measurements by Ying et al., or the calculated values in this study are most probably indicative of violations of the applied assumptions in the interpretation of RCSA data by Hansen and Al-Hashimi. For example, zero-point motion average bond lengths are substantially larger (r_{CH}(base) = 1.102 Å and $r_{C1'H1'}$(sugar) = 1.118 Å) than those used by Hansen and Al-Hashimi. The use of zero-point motion average bond lengths would result in reduced values of $|\sigma^{M}|$. On the other hand, these differences might also reflect genuine differences in aromatic carbon electron densities in mononucleosides and polynucleosides.

The only available experimental data on sugar carbon CSA in 2′-deoxynucleosides are for 2′-deoxythymidine (Stueber and Grant 2002). The calculated $|\sigma^{M}|$ values are in excellent agreement with the experimental results of Stueber and Grant. The calculated $|\sigma^{M}|$ values differ from

the previously reported experimental values by an average of 2.9 ± 2 ppm. Remarkably, the variations in sugar carbon MSA magnitudes, due to sugar repuckering, range between 5 and 35 ppm.

Not surprisingly, the sugar carbon MSA tensors for 2′-deoxynucleosides differ in absolute numbers from those in ribonucleosides (Table 2). However, it may be expected that sugar carbon MSA tensors in (poly)-ribonucleotides will exhibit similar patterns of conformational dependence on sugar pucker and glycosidic torsion angle. To illustrate this, we compared experimentally acquired polyribonucleotide λ values, defined as $\lambda = \frac{I^{\mathrm{CSA,DD}}_{\mathrm{C3'},\mathrm{C3'-H3'}}}{I^{\mathrm{CSA,DD}}_{\mathrm{C1'},\mathrm{C1'-H1'}}} \cong \frac{\sigma^*(\mathrm{C3'})}{\sigma^*(\mathrm{C1'})}$, where $\sigma^* = \sum_{i=1}^{3} \sigma^{\mathrm{C}}_{\mathrm{ii}} \left(\frac{3\cos^2\theta_{\mathrm{ii}}-1}{2}\right)$, $\sigma^{\mathrm{C}}_{\mathrm{ii}}$ is the ii-th component of the diagonalized C1′/C3′ CSA/MSA tensor, and θ_{ii} is the projection angle between C1′–H1′/C3′–H3′ dipole–dipole vector and principal axis of the CSA/MSA tensor, from Boisbouvier et al. (2000) with the λ values predicted by our calculations (Fig. 9). In their study, Boisbouvier et al. measured cross-correlated relaxation rates between C1′–H1′/C3′–H3′ dipole–dipole and C1′/C3′ chemical shift anisotropy in three model RNA polynucleotides.

They demonstrated that the ratio λ sensitively reflects differences in magnitude and orientation of the C1′/C3′ MS tensors between C2′-endo and C3′-endo sugar puckers, as originally suggested by Dejaegere and Case (1998). The sugar pucker in polyribonucleotides can be unequivocally assigned based on the λ values from calculated MSA tensors for 2′-deoxynucleosides (Fig. 9). This indicates that the differences in magnetic shielding due to sugar repuckering override those due to differences in the molecular structure of ribose and 2′-deoxyribose.

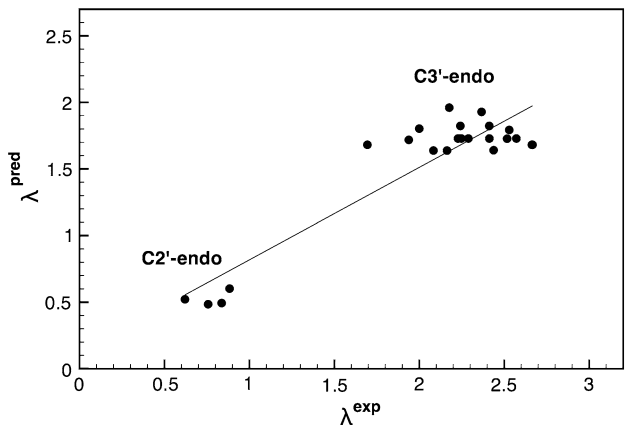

Fig. 9 Correlation plot between experimental $^{\mathrm{exp}}\lambda = \frac{I^{\mathrm{CSA,DD}}_{\mathrm{C3'},\mathrm{C3'-H3'}}}{I^{\mathrm{CSA,DD}}_{\mathrm{C1'},\mathrm{C1'-H1'}}} \cong \frac{\sigma^*(\mathrm{C3'})}{\sigma^*(\mathrm{C1'})}$ values acquired on three different RNA molecules by Boisbouvier et al. (2000) and those calculated based on C1′ and C3′ MSA tensors derived in present study (λ^{pred}). $\sigma^* = \sum_{i=1}^{3} \sigma^{\mathrm{C}}_{\mathrm{ii}} \left(\frac{3\cos^2\theta_{\mathrm{ii}}-1}{2}\right)$, where $\sigma^{\mathrm{C}}_{\mathrm{ii}}$ is the ii-th component of the diagonalized C1′/C3′ MSA tensor, and θ_{ii} is the projection angle between C1′–H1′/C3′–H3′ dipole–dipole vector and principal axis of the MSA tensor

In their original report, Boisbouvier et al. assigned $\lambda < 1.0$ and $\lambda > 2.0$ to C3′-endo and C2′-endo sugar conformations, respectively. Values of λ around 1.5 were assigned to sugars undergoing conformational averaging. For 2′-deoxyguanosine, our calculations suggest that λ values around 1.5 might alternatively be interpreted as indicating *syn* 2′-deoxyguanosine with C3′-endo sugar pucker.

In a recent report, Ravindranathan et al. (2005) characterized base carbon CSA tensors in an RNA kissing complex using both transverse and longitudinal auto- and cross-correlated relaxation rates. They found that the C2 and C8 CSA tensor magnitudes for residues in a stem differ from those in a loop region. Differences in $|\sigma^{\mathrm{M}}|$ of up to 14.2 ppm for adenosine and 19.4 ppm for guanosine residues were observed. However, these differences could not be attributed directly to either reorientation of the glycosidic bond (all residues in the loop as well as the stem are in the *anti* conformation) or internal dynamics. These results indicate that, in addition to the conformationally dependent variability of the MSA tensors and internal dynamics effects, there are other factors influencing actual MSA values. Extra care must be taken when interpreting MSA-related NMR parameters in the non-canonical region, as minute changes in hydration and/or accessibility of ion binding sites might also impact chemical shielding.

It follows that despite the good agreement of our calculated MSA values with experimental data, casual application of our calculated MSA values can still lead to biased assessment of the structural information. The accuracy of the calculated MSA tensor depends on the model compound and basis set used in the calculations. In order to assess MSA values correctly, the calculated points should be obtained from polynucleotide models in the explicit solvent and in the presence of ions. In practice, however, it is very difficult to satisfy such a requirement due to exorbitant computational time costs. Hence, evaluation of NMR observables based on calculated MSA values must be done with caution. On the other hand, the constant and systematic effect of the atomic basis on $|\sigma^{\mathrm{M}}|$ is less important for the prediction of its actual structural dependence since experimentalists are usually interested in relatively distinguishing between different conformers. The absolute correlation of experimental and theoretical values is the domain of methodological studies.

While finishing our calculations, we provided our preliminary data to the group of Prof. Harald Schwalbe for analysis of the temperature-dependent dynamics of RNA YNMG-tetraloops. Schwalbe and coworkers found that the χ-value dependence of the MSA needs to be considered in order to yield fully consistent results on order parameters

derived from ^{13}C relaxation rates or ^{15}N relaxation analysis (Ferner et al. 2008). Their results have clearly demonstrated that the conformation around the glycosidic torsion angle has a pronounced effect on the base carbon MSA that propagates into the order parameter analysis. Importantly, they showed that calculated MSA values, such as those generated here, can be used directly for correction of experimental ^{13}C and ^{15}N CSA values, facilitating an appropriate and physically meaningful model-free analysis.

Strictly speaking, the presented calculated MS-tensors parameters are approximate. A more quantitative analysis would have to respect dynamic effects, i.e., quantum-mechanical averaging of the MS-tensors over the bond lengths and bond angle fluctuations and torsional motions. So far, there are no data available on the effect of vibrational averaging on chemical shielding anisotropies in nucleic acids. However, Jordan et al. recently showed that the principal values and orientations of the ^{13}C carbonyl MSA tensor in peptides are very sensitive to small local changes in structure. In analogy to proteins, one might expect that the MSA tensors in nucleic acid will fluctuate as a function of time when bond lengths and bond and torsion angles fluctuate. Based on recent calculations by Jordan et al. (2007) and Tang and Case (2007), it is possible to estimate that the magnitude of static MSA tensors would be about 5–15% higher as compared with a vibrationally averaged, effective CS tensor derived from measurements in solution.

We showed that the use of the Iglo II basis in our calculation leads to systematic underestimation of the static MS tensor. In this respect, the virtual quantitative agreement between our calculated MSA values and those from relaxation and liquid crystal measurements might be considered as an artifact. The agreement between experimental and calculated values rather indicates that underestimation of the static MSA values due to the use of a small basis set in our calculations on average compensates for the neglected averaging effects.

Conclusion

In this study, we investigated the dependence of ^{13}C and ^{15}N MSA tensors in 2′-deoxynucleosides on the conformation of the glycosidic torsion angle and sugar pucker mode using DFT calculations. Contrary to the assumptions generally applied in structural interpretations of NMR parameters related to MSA, such as transversal and longitudinal auto- and cross-correlated relaxation rates and residual chemical shift anisotropies, our calculations indicate that the conformation of the glycosidic bond strongly influences C6/8 MSA tensors in 2′-deoxynucleosides. In light of the methods recently established for structural interpretation of base carbon RCSA (Grishaev et al. 2006; Hansen and Al-Hashimi 2006), we expect that the dependence of C6 and C8 CSA tensors on χ may adversely affect RCSA analysis and lead to errors in structure determination.

On the other hand, our calculations indicate that this dependence may be very useful for determining preferred glycosidic bond conformations. Based on our calculations, we propose to extend Hansen's and Grishaev's methods to quarternary C4 in 2′-deoxypyrimidines and to C4, C5, C6, and N7 in 2′-deoxypurines. In general, the use of conformation-specific MSA tensor values appears to be crucial for proper interpretation of NMR data related to MSA for both canonical and non-canonical nucleic acid structures. Good agreement of data calculated for 2′-deoxynucleosides with experimental data acquired on ribonucleosides and polyribonucleotides suggests that the conformational dependence of ^{13}C and ^{15}N MSA suggested by our calculations may be valid for polyribonucleotides as well.

Acknowledgements This study was supported by Ministry of Education of the Czech Republic grant no. MSM6007665801 and by the Academy of Sciences of the Czech Republic, grants no. IAA400550701/AV0Z50040507/AV0Z50040702 and KAN200100801. We thank Prof. H. Schwalbe for providing us with a manuscript (Ferner et al. 2008) prior to publication.

References

Akke M, Fiala R, Jiang F, Patel D, Palmer AG III (1997) Base dynamics in a UUCG tetraloop RNA hairpin characterized by 15N spin relaxation: correlations with structure and stability. RNA 3:702–709

Altona C, Sundaralingam M (1972) Conformational-analysis of sugar ring in nucleosides and nucleotides—new description using concept of pseudorotation. J Am Chem Soc 94:8205–8212

Becke AD (1993) A new mixing of Hartree-Fock and local density-functional theories. J Chem Phys 98:1372–1377

Boisbouvier J, Brutscher B, Pardi A, Marion D, Simorre J-P (2000) NMR determination of sugar puckers in nucleic acids from CSA-dipolar cross-correlated relaxation. J Am Chem Soc 122:6779–6780

Bryce DL, Grishaev A, Bax A (2005) Measurement of ribose carbon chemical shift tensors for A-form RNA by liquid crystal NMR spectroscopy. J Am Chem Soc 127:7387–7396

Czernek J, Fiala R, Sklenar V (2000) Hydrogen bonding effects on the (15)N and (1)H shielding tensors in nucleic acid base pairs. J Magn Reson 145:142–146

Dejaegere AP, Case DA (1998) Density functional study of ribose and deoxyribose chemical shifts. J Phys Chem A 102:5280–5289

Duchardt E, Schwalbe H (2005) Residue specific ribose and nucleobase dynamics of the cUUCGg RNA tetraloop motif by NMR 13C relaxation. J Biomol NMR 32:295–308

Duchardt E, Richter C, Ohlenschlager O, Gorlach M, Wohnert J, Schwalbe H (2004) Determination of the glycosidic bond angle chi in RNA from cross-correlated relaxation of CH dipolar coupling and N chemical shift anisotropy. J Am Chem Soc 126:1962–1970

Ebrahimi M, Rossi P, Rogers C, Harbison GS (2001) Dependence of 13C NMR chemical shifts on conformations of RNA nucleosides and nucleotides. J Magn Reson 150:1–9

Ferner J, Villa A, Duchardt E, Widjajakusuma E, Wohnert J, Stock G, Schwalbe H (2008) NMR and MD studies of the temperature-dependent dynamics of RNA YNMG-tetraloops. Nucleic Acids Res 36:1928–1940

Fiala R, Sklenar V (2007) 13C-detected NMR experiments for measuring chemical shifts and coupling constants in nucleic acid bases. J Biomol NMR 39:153–163

Fiala R, Munzarova ML, Sklenar V (2004) Experiments for correlating quaternary carbons in RNA bases. J Biomol NMR 29:477–490

Frisch MJ, Trucks GW, Schlegel HB, Scuseria GE, Robb MA, Cheeseman JR, Montgomery JA, Vreven T, Kudin KN, Burant JC, Millam JM, Iyengar SS, Tomasi J, Barone V, Mennucci B, Cossi M, Scalmani G, Rega N, Petersson GA, Nakatsuji H, Hada M, Ehara M, Toyota K, Fukuda R, Hasegawa J, Ishida M, Nakajima T, Honda Y, Kitao O, Nakai H, Klene M, Li X, Knox JE, Hratchian HP, Cross JB, Bakken V, Adamo C, Jaramillo J, Gomperts R, Stratmann RE, Yazyev O, Austin AJ, Cammi R, Pomelli C, Ochterski JW, Ayala PY, Morokuma K, Voth GA, Salvador P, Dannenberg JJ, Zakrzewski VG, Dapprich S, Daniels AD, Strain MC, Farkas O, Malick DK, Rabuck AD, Raghavachari K, Foresman JB, Ortiz JV, Cui Q, Baboul AG, Clifford S, Cioslowski J, Stefanov BB, Liu G, Liashenko A, Piskorz P, Komaromi I, Martin RL, Fox DJ, Keith T, Al-Laham MA, Peng CY, Nanayakkara A, Challacombe M, Gill PMW, Johnson B, Chen W, Wong MW, Gonzalez C, Pople JA (2004) Gaussian 03, revision C.02, Gaussian Inc., Pittsburgh, PA

Grishaev A, Ying J, Bax A (2006) Pseudo-CSA restraints for NMR refinement of nucleic acid structure. J Am Chem Soc 128: 10010–10011

Hansen AL, Al-Hashimi HM (2006) Insight into the CSA tensors of nucleobase carbons in RNA polynucleotides from solution measurements of residual CSA: towards new long-range orientational constraints. J Magn Reson 179:299–307

Hu J-Z, Facelli JC, Alderman DW, Pugmire RJ, Grant DM (1998) 15N chemical shift tensors in nucleic acid bases. J Am Chem Soc 120:9863–9869

Jordan DM, Mills KM, Andricioaei I, Bhattacharya A, Palmo K, Zuiderweg ER (2007) Parameterization of peptide 13C carbonyl chemical shielding anisotropy in molecular dynamics simulations. ChemPhysChem 8:1375–1385

Kutzelnigg W, Fleischer U, Schindler M (1991) The IGLO Meod: ab initio calculation and interpretation of NMR chemical shifts and magnetic susceptibilities. In: Diehl P, Fluck E, Günther H, Kosfeld R, Seelig J (eds) NMR basic principles and progress, vol 23. Springer, Heidelberg, pp 165–262

Lee CT, Yang WT, Parr RG (1988) Development of the Colle-Salvetti correlation-energy formula into a functional of the electron-density. Phys Rev B 37:785–789

Markley JL, Bax A, Arata Y, Hilbers CW, Kaptein R, Sykes BD, Wright PE, Wuthrich K (1998) Recommendations for the presentation of NMR structures of proteins and nucleic acids. J Mol Biol 28:933–952

Precechtelova J, Munzarova ML, Novak P, Sklenar V (2007) Relationships between 31P chemical shift tensors and conformation of nucleic acid backbone: a DFT study. J Phys Chem B 111:2658–2667

Ravindranathan S, Kim CH, Bodenhausen G (2003) Cross correlations between 13C-1H dipolar interactions and 15N chemical shift anisotropy in nucleic acids. J Biomol NMR 27:365–375

Ravindranathan S, Kim CH, Bodenhausen G (2005) Determination of 13C CSA tensors: extension of the model-independent approach to an RNA kissing complex undergoing anisotropic rotational diffusion in solution. J Biomol NMR 33:163–174

Schofberger W, Sychrovsky V, Trantirek L (2006) Quantum chemical calculations of NMR parameters. In: Sponer J, Lankas F (eds) Computational studies of RNA and DNA (Challenges and Advances in Computational Chemistry and Physics). Springer, Dordrecht, pp 513–536

Shajani Z, Varani G (2007) NMR studies of dynamics in RNA and DNA by 13C relaxation. Biopolymers 86:348–359

Sitkoff D, Case DA (1998) Theories of chemical shift anisotropies in proteins and nucleic acids. Prog NMR Spectr 32:165–190

Stueber D, Grant DM (2002) 13C and (15)N chemical shift tensors in adenosine, guanosine dihydrate, 2′-deoxythymidine, and cytidine. J Am Chem Soc 124:10539–10551

Sychrovsky V, Muller N, Schneider B, Smrecki V, Spirko V, Sponer J, Trantirek L (2005) Sugar pucker modulates the cross-correlated relaxation rates across the glycosidic bond in DNA. J Am Chem Soc 127:14663–14667

Tang S, Case DA (2007) Vibrational averaging of chemical shift anisotropies in model peptides. J Biomol NMR 38:255–266

Trantirek L, Caha E, Kaderavek P, Fiala R (2007) NMR (13)C-relaxation study of base and sugar dynamics in GCAA RNA hairpin tetraloop. J Biomol Struct Dyn 25:243–252

Wolinski K, Hinton JF, Pulay P (1990) Efficient implementation of the gauge-independent atomic orbital method for NMR chemical-shift calculations. J Am Chem Soc 112:8251–8260

Ying J, Grishaev A, Bax A (2006a) Carbon-13 chemical shift anisotropy in DNA bases from field dependence of solution NMR relaxation rates. Magn Reson Chem 44:302–310

Ying J, Grishaev A, Bryce DL, Bax A (2006b) Chemical shift tensors of protonated base carbons in helical RNA and DNA from NMR relaxation and liquid crystal measurements. J Am Chem Soc 128:11443–11454